CLASSIFYING FOREST AND NONFOREST LAND ON SPACE PHOTOGRAPHS

Robert C. Aldrich, Principal Research Forester

Pacific Southwest Forest and Range Experiment Station
Forest Service, U. S. Department of Agriculture
Berkeley, California

INTRODUCTION

One important function of the Nationwide Forest Survey[1/] is to keep forest area, volume and growth statistics up to date for the 509 million acres of commercial forest land in the United States. The present 5- to 10-year schedule for resurveys of the forest resources by states is too infrequent to keep up with the rapid changes that are occurring. Another handicap is the fact that regardless of inventory schedules, new forest statistics are never available for the entire Nation or for an entire state at one time. In other words, we have a continuous forest inventory system. Space-age remote sensing could help to keep these statistics up to date by monitoring the forest for changes--land-use changes or forest disturbances that affect timber volume and growth.

Before we can use new concepts in remote sensing on extensive forest surveys, dependable predictors of forest area, timber volume, and condition classifications must be developed. But this is really not a new problem--predictors have been used with panchromatic or infrared aerial photographs ever since they were first used on a timber survey more than thirty years ago. The difference is that today we have a wider variety of sensors,

---

1/ The Forest Survey is a branch in the Division of Forest Economics and Marketing Research, Forest Service, U. S. Department of Agriculture, Washington, D. C. The Forest Survey was authorized by the McSweeney-McNary Forest Research Act of May 22, 1928.

including color, infrared color, and multiband photography, which require new ideas and a completely different approach to image analysis.

Because of this need, the Forest Service Remote Sensing Research Project at Berkeley, California, began a program to seek solutions to forest inventory problems using new remote sensing tools. This research is supported by funds from the Forest Service, U. S. Department of Agriculture and the National Aeronautics and Space Administration. Our objectives were: to determine the limits of accuracy for forest area estimation on space photography, to determine the feasibility of using space photography to detect and outline disturbances in forest communities, and to develop spectral signatures for forest and land-use classes that may be related to Earth Resources Technology Satellites (ERTS) data. Some of the most significant results of this study will be reported here.

THE STUDY AREA

The study area is located southwest of Atlanta, Georgia, and is one of two areas used in the forest inventory study reported by Langley (1) a year ago (Fig. 1). We selected this area for several reasons, not the least of which is the excellent photographic coverage provided by Apollo 9 in March 1969. Another important reason is the geographic location. This area lies in one of the best timber growing regions of the country with diversified forest types and many different growing conditions. Furthermore, a wide variety of industries, including manufacturing, agricultural cash crops, livestock, and forest industry support the local economy. As a result, many land-use patterns and land-management practices present a challenge to remote sensing. The nearness of Atlanta, the transportation hub of the South, makes this area extremely accessible and subjects the area to changes created by a growing urban environment.

Our final reason for selecting this area was the result of our 1969 multistage forest inventory study. By studying this area in greater depth, we hope to improve predictions for volume stratification on space photographs which will lead to greater sampling efficiency.

This area is located in the southern piedmont land resources subregion (2). It is about 60 percent forested, mainly in farm woodlands. The elevations range from about 250 meters (800 feet) in the southeast to 400 meters (1300 feet) in the northwest. The topography is gently rolling to hilly and is cut by many narrow stream bottoms. Mean annual rainfall is approximately 125 centimeters (50 inches). The soils are primarily red and yellow podzolics. Major forest types in this region are loblolly-shortleaf pine and oak-pine (2). In addition to loblolly *(Pinus taeda)*, shortleaf *(Pinus echinata)*, and other southern pines, several oaks *(Quercus* sp.*)*, hickories *(Carya* sp.*)*, yellow poplar *(Liriodendron tulipifera)*, black gum *(Nyssa sylvatica)*, and sweet gum *(Liquidambar styraciflua)* are plentiful in a variety of mixtures.

REMOTE SENSOR DATA ACQUISITION

Since March 1969 we have accumulated an assortment of remote sensor data to support this study. These data range all the way from 1:2,000 color transparencies to the Apollo 9 space photographs. A review of these data seems essential at this time.

FOREST SERVICE PHOTOGRAPHY

In April 1969 the Forest Service remote sensing aircraft flew multi-scale photography for five 6.4-kilometer (4-mile) square blocks used in the 1969 inventory study (Fig. 2). This consisted primarily of 70 mm. photography for randomly selected sample strips. The photographic data are shown in Table 1. The high-quality large-scale color photographs have been useful in establishing land use and forest classifications at the time of the Apollo 9 flight. Small-scale Polaroid and Aero Neg color have been useful for planning and directing field crews to ground locations.

In March of this year, almost one year following the Apollo 9 flight, we rephotographed each of the five study blocks using Ektachrome infrared color film (8443) at a 1:32,000 scale. We also photographed one of the random sample strips with Eastman Aero Neg color film at a 1:12,000 scale. Ten additional 6.4-kilometer (4-mile) square blocks were selected at random and photographed at this same time. These new blocks will be used in the next phase of the study to test interpretation training models as they are developed.

The 1:32,000 IR color photography and ground observations are being used to check photo classification made by both manual and automated interpretation techniques on small-scale simulated space photography provided by RB-57 high-altitude flights.

NASA RB-57 PHOTOGRAPHY

In June 1970 we acquired our first coverage of the Atlanta test site by an RB-57 high-altitude flight (Mission #131). The entire test site was covered in seven flight lines (Fig. 3). For this mission we requested and received the data described in Table 2.

Copies of the Mission 131 data were received on July 30--8 weeks following the flight. In terms of coverage the flight was successful. Of the fifteen 6.4-kilometer (4-mile) square study blocks, all but one was completely covered by the smallest scale photography. Unfortunately, this block was one of five intensive study blocks to be used in developing training models. Four of the five blocks were covered by the 1:120,000 scale RC-8 Ektachrome photography. Only one block was entirely covered by the largest scale Zeiss photography; but this was to be expected due to the limited side lap with this camera.

Of all the data received, only the RC-8 Ektachrome film taken with a 425 mμ filter and the panchromatic and B/W infrared Hasselblad films were completely acceptable for our purposes. Poor filter selection and poor film manufacture can be blamed for the failures of the Ektachrome with a 450 mμ filter and the infrared color films taken with both the Zeiss and Hasselblad cameras.

PHOTO ANALYSIS

Both satellite and small-scale aerial photography require special techniques for data analysis. In this section we will discuss some of the techniques we used to overcome the problems of interpreting coarse resolution imagery.

FOREST AREA PREDICTIONS

The Apollo 9 space photographs were taken in March and provided some helpful characteristics to separate forest land from nonforest land (3).

First, the deciduous tree species (hardwoods) were without leaves. This resulted in a distinctive bluish green color that allows interpreters to evaluate where deciduous trees predominate. The contrast between bluish green deciduous forest and medium to dark purplish red evergreen (pine) forest separates these two pure types and helps to identify where mixtures of both pines and hardwoods occur. Another advantage to March photography is the absence of crops on the greater part of the active agriculture land. Although fields had been plowed in preparation for planting, it was evident that few crops other than overwintering grains and pasture were present. This made it possible to separate forest from a large portion of the nonforest land.

One important limitation of space photographs is the poor ground resolution. On the Apollo 9 IR color we found that the resolution was approximately 91 meters (300 feet). Thus, small fields in dark forested areas and small farm woodlots in lighter toned agricultural areas were not resolved. Although the human eye cannot resolve these small features, there is hope that microdensitometers may detect minute differences in color density and recognize spectral signatures for land-use classification (4) (5).

Another limitation of satellite photography taken in March is the high ground water level resulting from winter and spring rains. High soil moisture and extremely high humus content of bottomland soils cause darker than normal images that may be mistaken for forest.

Using these criteria for interpretation, photo interpreters estimated the forest area within the five random 6.4-kilometer (4-mile) square study blocks on the Apollo 9 IR color film. Because of the small image size (6.4 kilometers equals 2.7 mm. on the photo), a Bausch and Lomb Zoom 70 stereoscope was used with 7.5X magnification (Fig. 4). Although there is little or no stereoscopic effect, we viewed images on adjacent photographs simultaneously. The two images viewed together complemented one another and aided the interpretation.

To check forest area predictions made on the space photograph, photo interpreters estimated the area of forest and other land-use classes on conventional medium-scale photography. Two sets of photographs were interpreted--the latest 1:20,000 Department of Agriculture (ASCS) panchromatic photography and 1:32,000 IR color photographs. The estimates were made using dot grid templates constructed to sample at an intensity of approximately 6.4 hectares (16 acres) per dot. This is more than 10 times the intensity used by the U. S. Forest Service to estimate forest area on their nationwide forest survey. An Old Delft scanning stereoscope was used to aid in this interpretation.

FOREST MAPPING

We selected one block (Block 3) to check the Apollo 9 forest proportion and to explore the possibility of mapping broad forest types and nonforest classes on low-resolution photography. We examined Block 3 on the Apollo 9 IR color transparency using 7.5X magnification. Then using a 28X panchromatic print enlargement made from the same photograph as a base map, we constructed a forest-type land-use map (Fig. 5). A dot grid was constructed to sample approximately 6.4 hectares (16 acres) per dot. Using this grid, the percent forest was estimated in three broad types: pine, upland hardwood, and bottomland hardwood. The percentage of the area in nonforest and water was also calculated. These data have been compared with estimates made on medium-scale conventional photography.

FILM DENSITY CLASSIFICATION

A Photometric Data Systems microdensitometer was used to measure and record optical density along randomly selected sample strips on the Apollo 9 IR color transparency (Fig. 6). The strips were first located on the 1:32,000 IR color transparencies taken in March 1970. These strips are between 6.4 kilometers (4 miles) and 8 kilometers (5 miles) long and will be used to develop signatures to be used in interpretation training models. Well-defined beginning and ending points were selected for each strip so that they could be transferred to both the Apollo 9 transparency and 1:400,000 scale photography supplied by NASA's high-altitude aircraft.

Two interpreters classified and delineated nine nonforest and four forest classes along each of the fourteen lines, Table 3. These delineations were marked on a transparent overlay as shown in Figure 7. An Old Delft scanning stereoscope with 4X magnification was used to assist in the classification. We also estimated crown closure for forest in three classes, and forest disturbances were classified into 10 classes. To help detect disturbances we compared each strip with the 1:12,000 photography taken in April 1969. When completed, the total length of line and length of each land-use segment along the line was measured and recorded to the nearest 100th millimeter. There were over 800 segments delineated on over 96 kilometers (60 miles) of line.

We selected 107 segments from all forest and agricultural categories for ground observations. The number selected in each category was arbitrarily set to obtain a representative sample of each. Ground observations were made between June 8 and June 18, 1970. Forest points were given a type designation based on an estimate of basal area per acre by tree species. Crown closure (density) was assigned to each point by ocular estimate, and stand size was based on an estimated number of sawtimber, pole, and seedling and sapling size trees. In addition, each part of the forest floor was examined and classified into seven classes. Munsell color standards[2/] were used for soil color classification. If we found a point that had been disturbed since March 1969, this was identified and recorded by cause.

Agricultural points were examined and classified by crop type and maturity, soil color, and erosion. Pasture land, idle land, and abandoned agriculture were classified by broad vegetation types, degree of grazing, erosion, and soil color. Both a 35 mm. color and infrared color photograph were taken on each forest and agricultural point to illustrate the conditions that we described.

[2/] Munsell Color Company. Munsell Book of Color. Ed. 1920-60. Baltimore, Md.

Using ground truth, the photo interpretation along the sample strips was adjusted to give a true picture of ground conditions. These adjusted photo data are known as our ground truth and are used to develop optical density signatures with an automatic scanning microdensitometer.

Using the microdensitometer, we scanned the 14 strips on Apollo 9 IR color frames 3791 and 3792. Because of the extremely small scale of this photography, we found that it was difficult to position the sample strips precisely for scanning. For this reason we developed a different technique. First we read the X and Y coordinates for the starting and ending points that we had selected and recorded them on tape. Then we programmed the microdensitometer to block-scan an area that included these two points. We used an effective aperture area of 18.67 μm and the microdensitometer was programmed to read at 9 μm intervals on scan lines 9 μm apart. The density readings along our sample line were determined by computer programming. The red, green, and blue mean densities and their standard deviations were computed for each land-use class by strips, blocks, and the sum of all blocks. These densities have been plotted for comparison.

We have not attempted to detect forest disturbances using the microdensitometer and automatic data processing. However, we did run a test on two areas with known disturbances. One is a stand of pine pulpwood that was cut sometime between April 1969 and March 1970. The other is a natural gas pipeline that was constructed during the same period. First, we selected beginning and ending points for scan lines that would pass through these two areas. These points had to be recognizable on a small-scale

Apollo 9 IR color and June RB-57 Hasselblad imagery. Then these two films were scanned and density read using red, blue, and green cutoff filters.

RESULTS

When forest area predicted on Apollo 9 photographs was compared with forest area estimated on medium-scale aerial photographs, we found some interesting relationships. Despite the differences in scales, estimates of forest area made on the Apollo 9 photograph are correlated to some degree with estimates on 1:32,000 IR color made a year later (Table 4). Only in Blocks 3 and 4 does the difference exceed 10 percent. On Block 4, the difference can be explained in part by the lack of full coverage on the 1:32,000 photography. Unfortunately the western quarter of the block was not covered.

The forest area in Block 3 was underestimated. This was verified by comparing the prediction with the mean of the other three estimates--the mean is 85 percent or 12 percent above the Apollo 9 prediction. To check this, a dot count was made on a forest-type land-use map constructed from the Apollo 9 photograph. This new prediction resulted in a forest area estimate of 80 percent and compares more favorably with the mean for the other three methods.

When we compare Block 3 area percentages by broad forest types there is some correlation between the Apollo 9 and the other two estimates (Table 5). All three scales resulted in bottomland hardwood estimates within one percent. Water estimates are extremely close. The estimate of pine type on the 1:32,000 IR color and Apollo 9 IR color were closer than we expected; the space photograph underestimated pine type by 15 percent. The estimate of pine type on the 1:20,000 panchromatic photography has obviously been affected by poor type discrimination on this film. Also, of the three estimates this was made by the least experienced interpreter. Better instruments for viewing and drawing maps directly from this extremely small-scale photography should improve these results.

Figure 8 shows a comparison of optical density for the thirteen forest and nonforest classes on Apollo 9 IR color photography. There were 4,985 data points involved in this analysis; 3,425 forest and 1,560 nonforest. Since we have used separate scans for red, green, and blue optical density this means that three times this number of data points were analyzed in the experiment.

Using density alone, our data indicate that at a confidence limit of one standard deviation (68 percent) we can discriminate between forest land and agricultural crops, plowed fields, pasture land, idle land, orchards, and turbid water. None of the three bands (red, green, or blue) appears to be better than another. Although at first glance the red band appears to have greater differences, the standard deviations for red density are greater than either green or blue. This would compensate for the greater density range shown in the curves.

Forest types cannot be separated based on density alone. The standard deviations about the means for density in all three bands overlap and reduce the probability of correct interpretation. However, the data do suggest that it may be possible to develop signatures for forest types, abandoned agriculture, urban and clear bodies of water using a combination of nine variables. These would include density, differences in density, and density ratios. For instance, the relationship of red density to blue and green density appears to provide a signature for recognizing forest from crops, plowed fields, idle, abandoned, orchard, urban areas and turbid water.

Phenological development of vegetation and sun altitude will affect spectral reflectance and the response of film emulsions. Thus, it is important to study these effects so that imagery from the Earth Resources Technology Satellites (ERTS), in 1972, can be selected to provide the type of information desired. The Earth Resources Program at NASA's Manned Spacecraft Center in Houston, Texas, is providing high-altitude multiband imagery for studies of this nature.

We have just begun to process multiband imagery taken from 18,288 meters (60,000 feet) by high-altitude aircraft from NASA's Manned Spacecraft Center in Houston. This is the first in a series of photographic flights that will include early summer, late summer, fall, and winter conditions. The first films to be processed were taken in June 1970. Only one (Block 5) has been completed. Since this block is 90 percent forested it is not a good example for land-use discrimination. However, it does show discrimination possibilities between forest types.

We processed the IR color film with a red, green, blue, and clear filter only using the same scanning procedure as described for the Apollo 9 films. The only difference is that we used a 99.17 mμ effective aperture size to scan approximately the same strip width in terms of ground resolution. Our data were collected at 51 μm intervals of scans 51 μm apart.

Figure 9 shows a comparison of red, green, and blue optical density measured on 1:420,000 infrared color film. Comparing these results with densities from Block 5 on the Apollo 9 infrared color film shows some interesting differences. The three-month difference in vegetation development between photography dates accounts for the big increase in red density levels (infrared response). Obviously, June photography with greater leaf cover should have a higher red density than March photography when deciduous trees are leafless, most vegetation is still dormant and solar radiation is still rather low by comparison. It is interesting to note the similarity in shapes of the two sets of curves. Although these data are encouraging, we can attach very little significance to them because the RB-57 IR color film was of such poor quality. However, our conclusions based on these data are the same as those for the Apollo 9 density scans. That is, density alone may discriminate forest from several nonforest classes, but to discriminate forest, forest types, and all nonforest classes will require combinations of density and between-density relationships.

The microdensitometer scans made on three different B/W infrared and panchromatic film and filter combinations resulted in the mean densities plotted in Figure 10. We do not show the densities for infrared film with a Wratten 12 filter and panchromatic film with a Wratten 12 filter because they appear to provide very little information for this study. It is obvious from the three curves that the infrared film with a Wratten 89B filter shows limited value for forest-nonforest discrimination by itself. Future analyses may show, however, that this film, when coupled with infrared color film, will aid in differentiating between bodies of water and forest. Although we have no data at present to support this point, an examination of the photographs shows that bodies of water are enhanced on this film. This has been a weakness of the IR color film taken from space. Bodies of water in dark forested backgrounds are not resolved.

Of the two panchromatic film-filter combinations shown, only the panchromatic with a 25A filter indicates any potential for land-use classification. Here again, the discrimination of urban areas may be aided if this film is used in concert with the IR color film. The better resolution capabilities of this film-filter combination may aid in resolving narrow urban features such as highways, pipelines, and power lines that are not resolved on the infrared color taken from space altitudes.

Detecting and measuring changes in the forest environment created by urban development and other manmade and natural causes is important to keep forest information up to date. The microdensitometer scans in Figure 11 are meant to demonstrate the feasibility of automatic scanning microdensitometers to detect a pulpwood cutting by repetitive satellite imagery. We used red density on the Apollo 9 IR color and blue density on the RB-57

IR color because they appeared to show the best discrimination.

The photographs in Figure 11 show the pulpwood stand before cutting and after the cutting. Some of the differences in the shapes of the two curves can be attributed to film resolution as well as seasonal responses for vegetation on IR color film. Despite these differences, there is certainly a noticeable response at the site of the pulpwood cutting.

Figures 12A and 12B show a similar demonstration for a pipeline location. Although we have much to learn about how to interpret these data by data processing, it does show some hope for detecting areas of forest change even on satellite imagery.

CONCLUSIONS

Although the research reported here is in its preliminary stages, we can make four rather broad statements regarding the results of this work.

1. Infrared color film is the best single multiband sensor available at the present time.

2. There is very good possibility that we can separate forest from all nonforest land uses by microimage evaluation techniques on IR color film coupled with B/W infrared (Wratten 89B filter) and panchromatic film (Wratten 25A filter).

3. Discrimination of forest and nonforest classes may be possible by either of two methods: (1) interpreters with appropriate viewing and mapping instruments might simultaneously view enlarged multiscaled images and map forest types and land uses for estimating acreages or (2) programmable automatic scanning microdensitometers and automatic data processing

techniques may be used to make land-use decisions based on optical densities, density differences and density ratios.

4. Results show the importance of procuring the best possible remote sensor data that are possible. Without good data our efforts can be of little significance.

Our plans for the next year include continued efforts to develop optical density signatures for forest and nonforest classes on Apollo 9 photography. Signatures developed for IR color, panchromatic (Wratten 25A filter), and B/W infrared (Wratten 89B filter) will be compared with signatures developed for RB-57 high-altitude photography for three seasons and 1:32,000 IR color taken in March 1970. We will also study the use of several pattern recognition techniques using these density signatures.

ACKNOWLEDGEMENTS

The work reported here would not have been possible without the assistance of Wallace Greentree, forester, who was responsible for the precise microdensitometer measurements and who ably assisted in all phases of the photo interpretation and field work; Mrs. Nancy X. Norick who provided guidance in the statistical approaches to image recognition; and Miss Marilyn Wilkes who did the computer programming.

LITERATURE CITED

1. Langley, P. G. R. C. Aldrich and R. C. Heller. 1970. Multi-stage sampling of forest resources by using space photography--an Apollo 9 case study. Second Annual Earth Resources Aircraft Program Status Review. Vol. 2. NASA, Manned Spacecraft Center, Houston, Texas. 28 pp., illus.
2. U. S. Forest Service. 1969. A forest atlas of the South. Southern Forest Experiment Station, New Orleans, La., and Southeastern Forest Experiment Station, Asheville, N. C. 27 p., illus.
3. Aldrich, R. C. 1970. Space photographs separate land use and aid in forest inventories. Paper presented at the 1970 joint annual meeting of ACSM and ASP, Washington, D. C. Submitted for publication in Photogramm. Engng. 30 pp., illus.
4. Doverspike, G. E., F. M. Flynn, and R. C. Heller. 1965. Microdensitometer applied to land use classification. Photogramm. Engng. 31(2):294-306.
5. Richardson, A. J., R. J. Torline, D. A. Weber, R. W. Leamer, and C. L. Weigand. 1970. Computer discrimination procedure comparisons using film optical densities. SWC Research Report 422. Rio Grande Soil and Water Research Center, Soil and Water Conservation Research Division Agricultural Research Service, U. S. Department of Agriculture, Weslaco, Texas. 39 pp., illus.

Table 1. Camera, focal length, film-filter data, scale and type of coverage for Apollo 9 forest inventory study support photography; April 1969.

Camera	Focal Length (mm.)	Film	Filter	Scale	Coverage
Crown Graphic	75	Polaroid 400	Wratten 12	1:60,000	Block (5)
Maurer KB-8	38	Eastman Aero Neg	HF-3	1:120,000	Block (5)
Maurer KB-8	228	Ekta IR color	Wratten 15	1:20,000	Strip (5)
Maurer KB-8	38	Eastman Aero Neg	HF-2	1:12,000	Strip (10)
Maurer KB-8	228	Ansco D/200	1A	1:2,000	Strip (174 sample triplets)

Table 2. Camera, focal length, film-filter, and photographic scale for RB-57 (Mission 131) photography for site 217, Atlanta, Georgia; June 1970.

Camera	Focal Length (mm.)	Film	Filter	Approximate Scale
RC-8	152	Ektachrome SO-397	450 mμ.	1:120,000
RC-8	152	Ektachrome SO-397	425 mμ.	1:120,000
Zeiss	305	Ektachrome IR SO-117	530 mμ.	1:60,000
Hasselblad	40	Panchromatic 2402	Wratten 25A	1:420,000
Hasselblad	40	Panchromatic 2402	Wratten 58B	1:420,000
Hasselblad	40	Panchromatic 2402	Wratten 12	1:420,000
Hasselblad	40	B/W IR, 2424	Wratten 89B	1:420,000
Hasselblad	40	B/W IR, 2424	Wratten 12	1:420,000
Hasselblad	40	Ektachrome IR SO-117	Wratten 15	1:420,000

Table 3. Land use and forest condition classification

Land Use	Code	Forest Condition	Code
Forest		Forest Density	
Pine (51-100% pine)	01	75-100 percent	1
Pine-Hardwood (25-50% pine)	02	25-75 percent	2
Bottomland Hardwood (0-25% pine)	03	0-25 percent	3
Upland Hardwood (0-25% pine)	04	Forest Disturbance	
Agriculture		No disturbance	01
Crops	05	Cutting - heavy	02
Plowed fields	06	Cutting - light	03
Pasture	07	Land clearing	04
Idle	08	Insect damage - heavy	05
Abandoned	09	Insect damage - light	06
Orchard	10	Disease damage - heavy	07
Urban	11	Disease damage - light	08
Water		Fire damage - heavy	09
Turbid	12	Fire damage - light	10
Clear	13		

Table 4. Comparison of percent forest area by study block, mean for all blocks, and type of photography.

Photography	Percent Forest Area					
	Block					Mean
	1	2	3	4	5	
	Percent					
Panchromatic 1/ (1:20,000)	77	36	81	45	85	65
Polaroid 2/ (1:60,000)	69	25	87	51	93	65
IR Color 1/ (1:32,000)	83	39	86	68	86	72
Apollo 9 2/ (1:2,430,000)	80	35	73	55	96	68

1/ Estimated from a count of over 600 photo points systematically located within each block.

2/ Ocular estimate.

Table 5. Comparison of area for forest and nonforest classes using three photo scales[1/]--Block 3.

Photography	Pine	Hardwood		Nonforest	Water
		Upland	Bottomland		
			Percent		
Panchromatic (1:20,000)	17.0	54.1	9.8	18.9	0.2
IR Color 1:32,000)	59.4	16.7	10.1	13.2	0.6
Apollo 9 (1:2,430,000)	44.8	24.2	10.7	19.7	0.6

[1/] Estimated from a count of over 600 photo points.

36-24

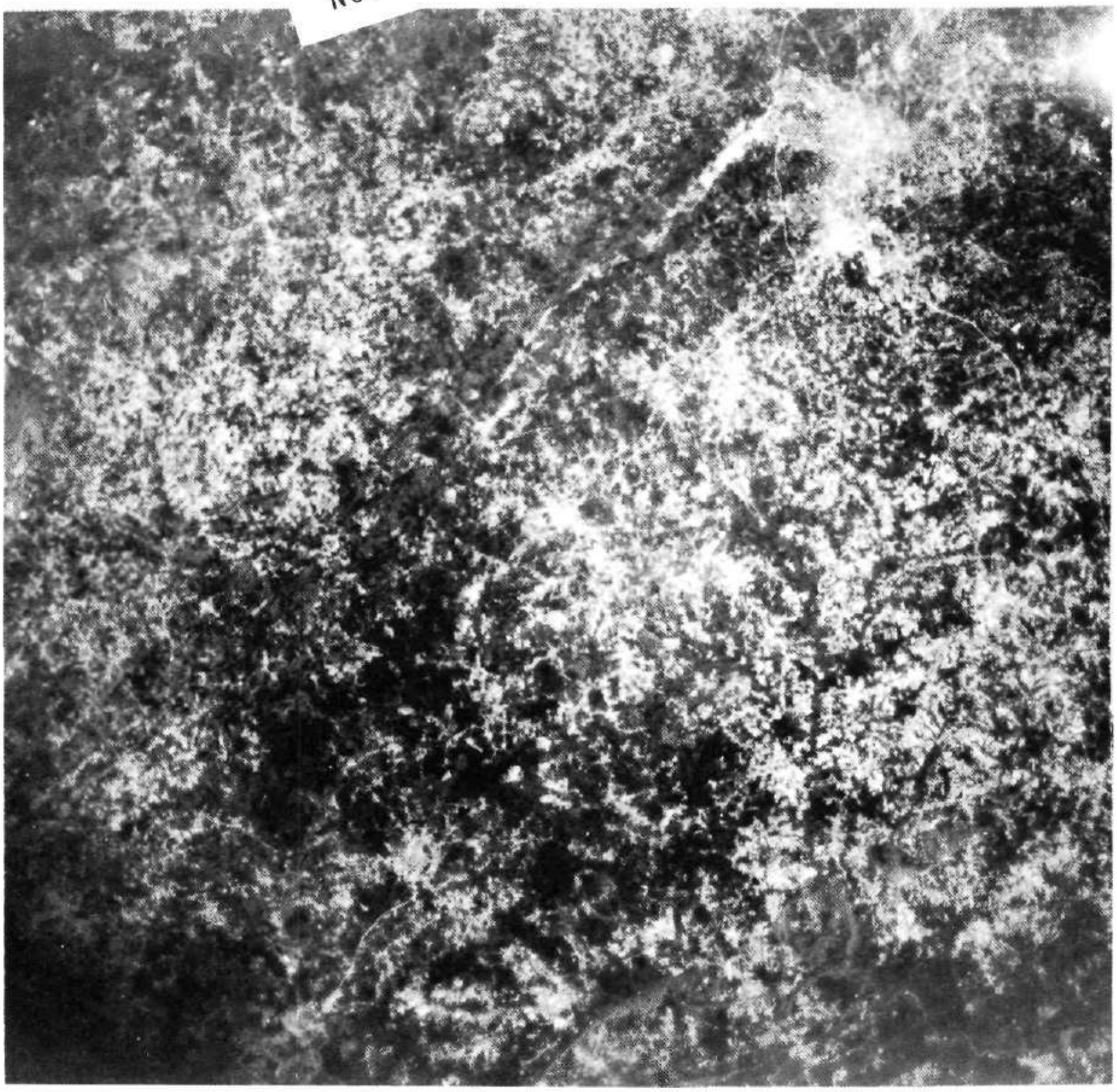

Figure 1.--Apollo 9 coverage for a portion of the Atlanta test site (Site 217). The light gray area in the upper right corner is Atlanta, Georgia. This photo was made from an IR color transparency.

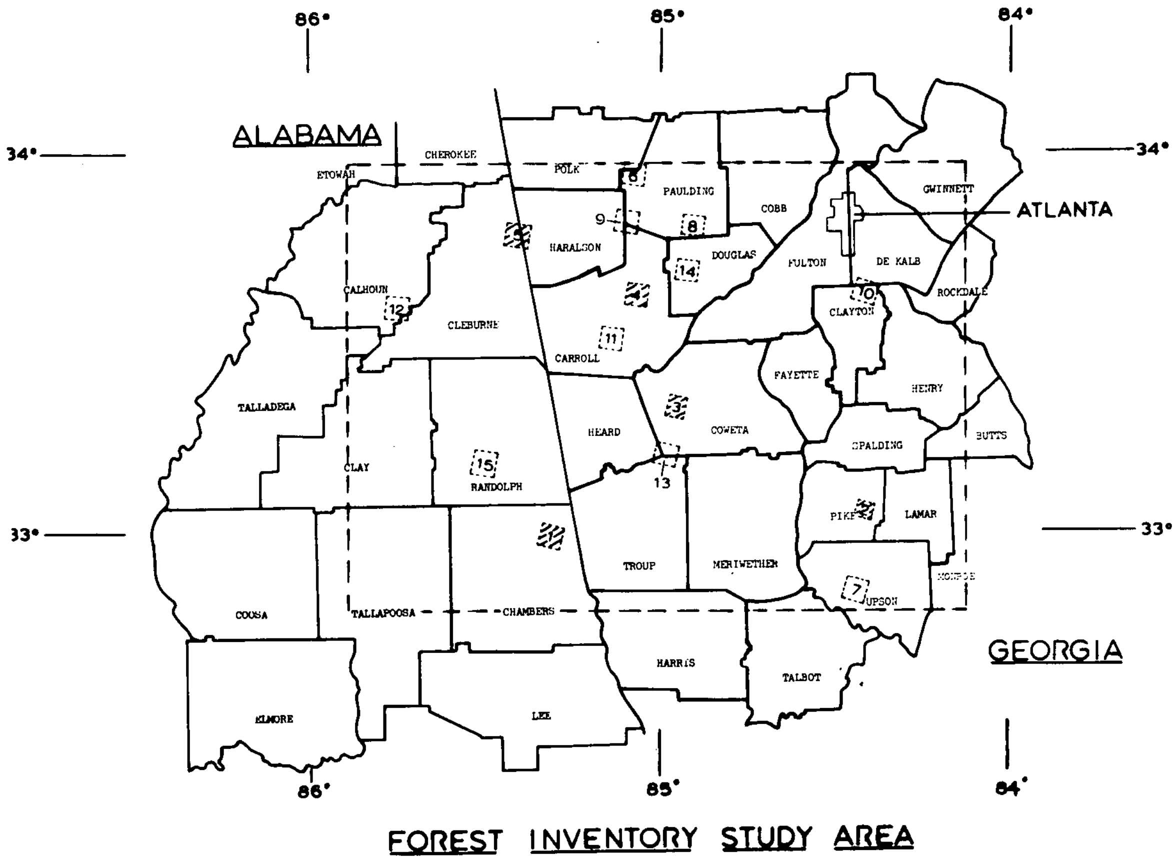

Figure 2.--The Atlanta test site includes all or portions of 27 counties in Alabama and Georgia. Five intensive study areas are shown with hatch marks. The 10 additional squares will be used to test interpretation models in another phase of this study.

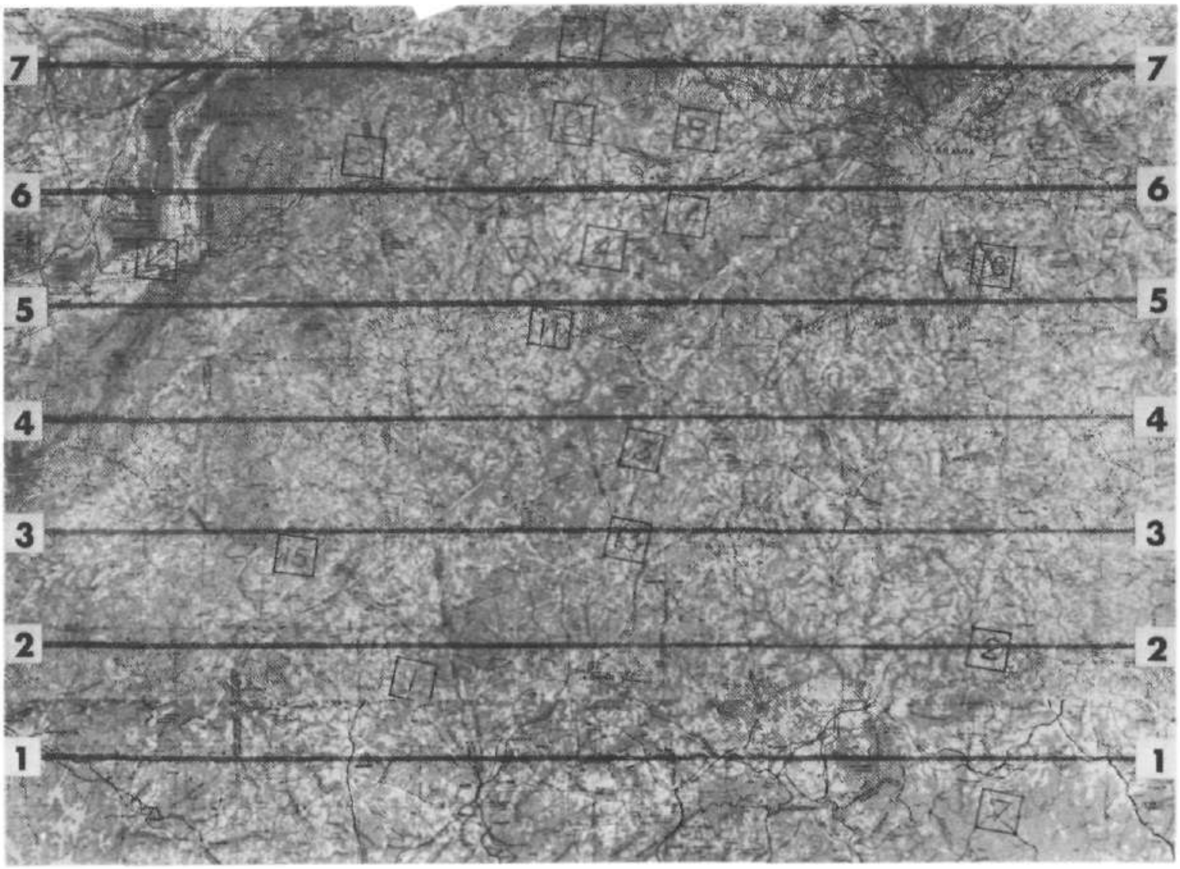

Figure 3.--RB-57 Mission 131 covered the Atlanta test site in 7 flight lines.

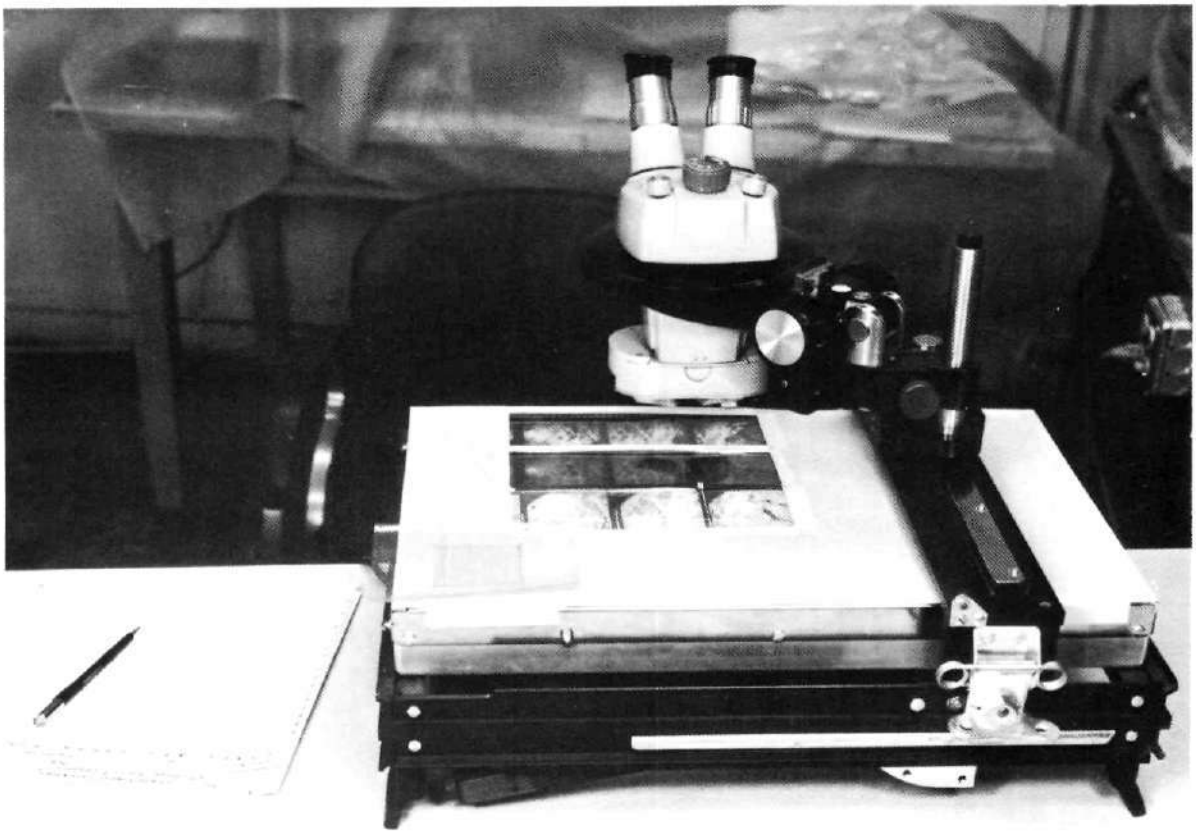

Figure 4.--Interpreters used a Bausch and Lomb Zoom 70 stereoscope at 7.5X to interpret satellite photography.

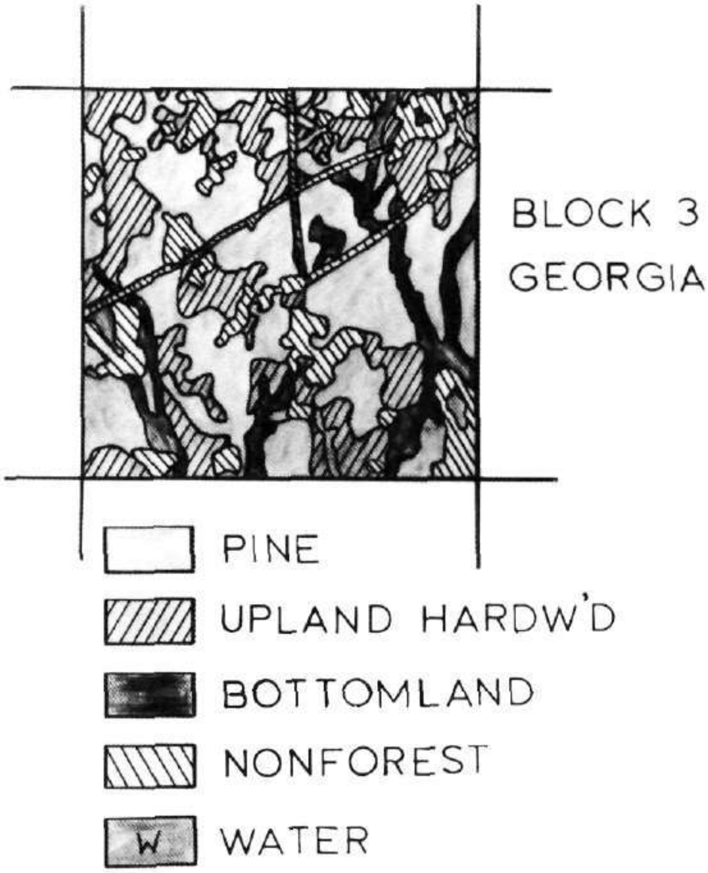

Figure 5.--A forest-type land-use map was constructed using a 28X enlargement of Block 3 made from the Apollo 9 IR color as a base map.

Figure 6.--A Photometric Data Systems microdensitometer coupled to a Data Acquisition System digitizer was used to scan the Apollo 9 and high-altitude RB-57 photography.

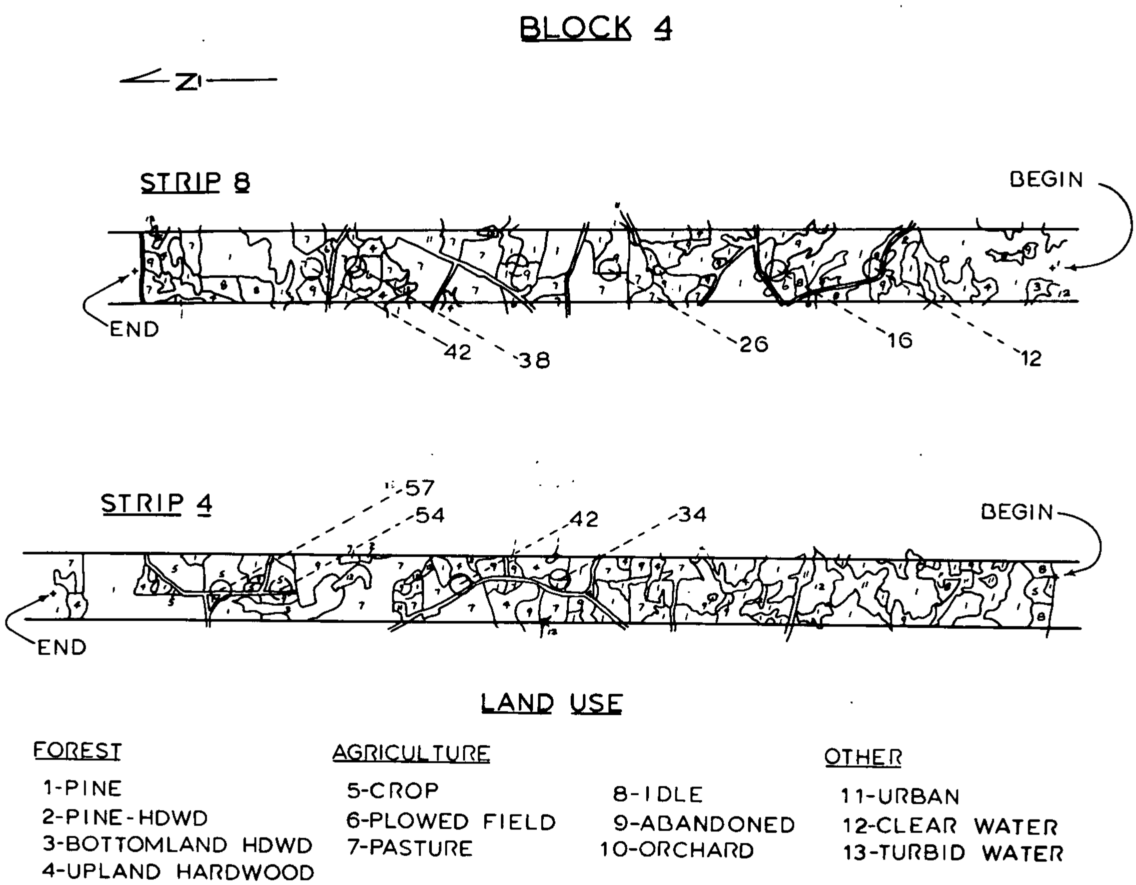

Figure 7.--Interpreters delineated forest type and land use along sample strips. These strips, adjusted by ground observations, are used as ground truth for microdensitometer scans on satellite and small-scale aerial photographs. Note beginning and ending points for the microdensitometer scans.

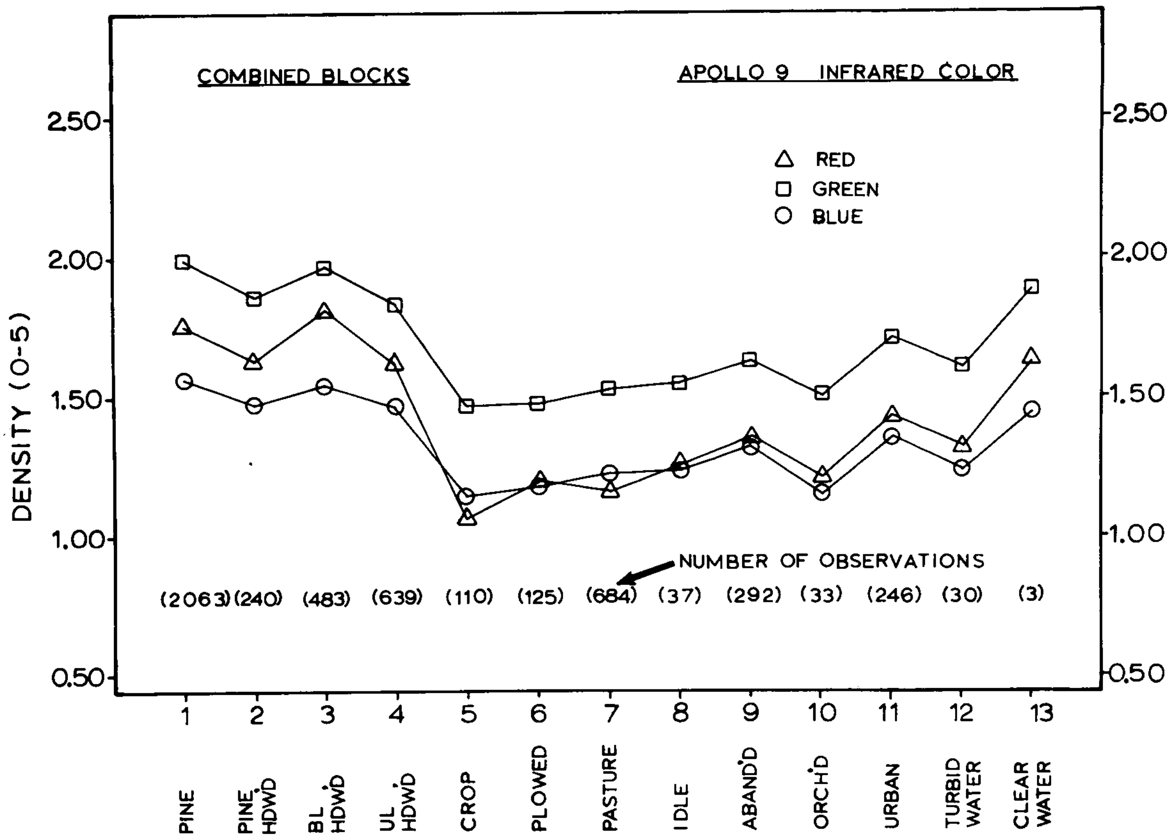

Figure 8.--The mean red, green, and blue optical densities for 13 forest and nonforest classes on Apollo 9 IR color--combined for all blocks.

A

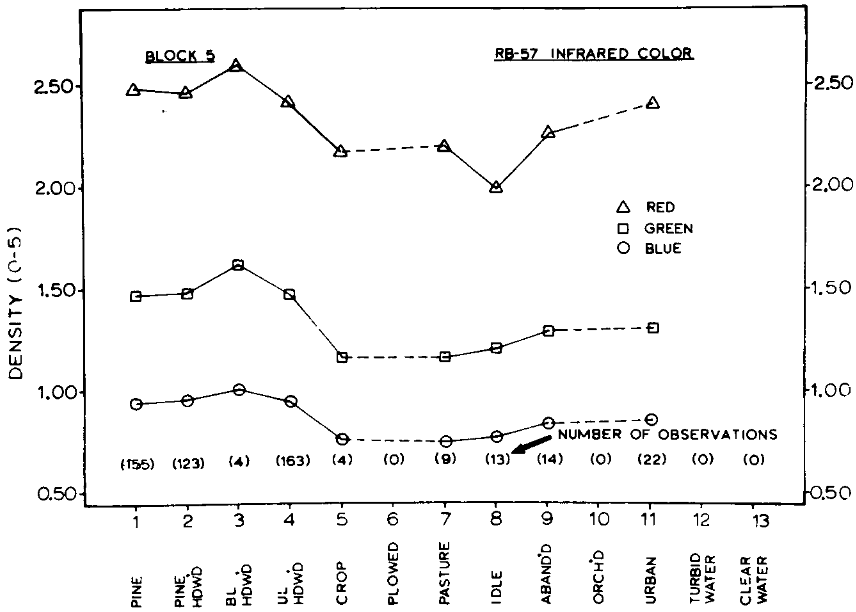

B

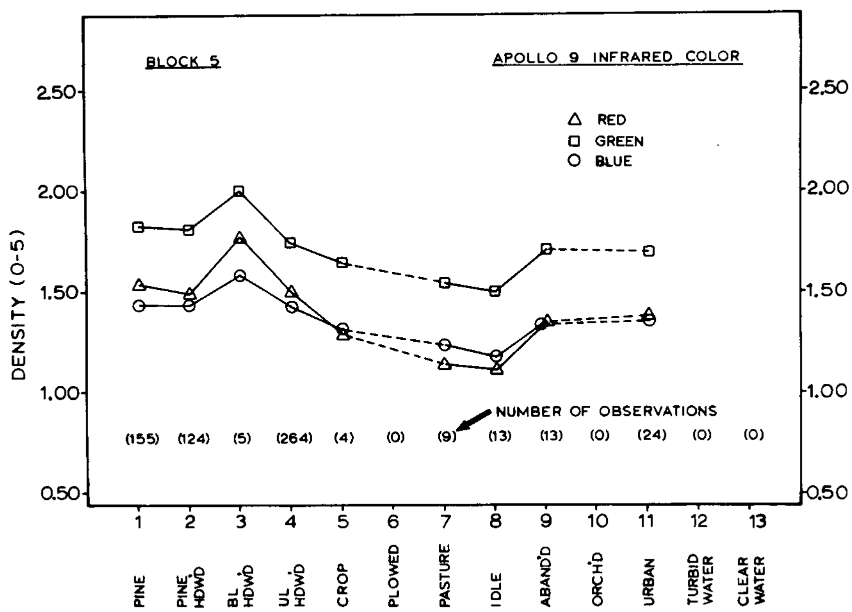

Figure 9.--The mean red, green, and blue optical densities for 9 of 13 forest and nonforest classes: (A) 1:420,000 IR color high-altitude photography, (B) Apollo 9 IR color--Block 5 only.

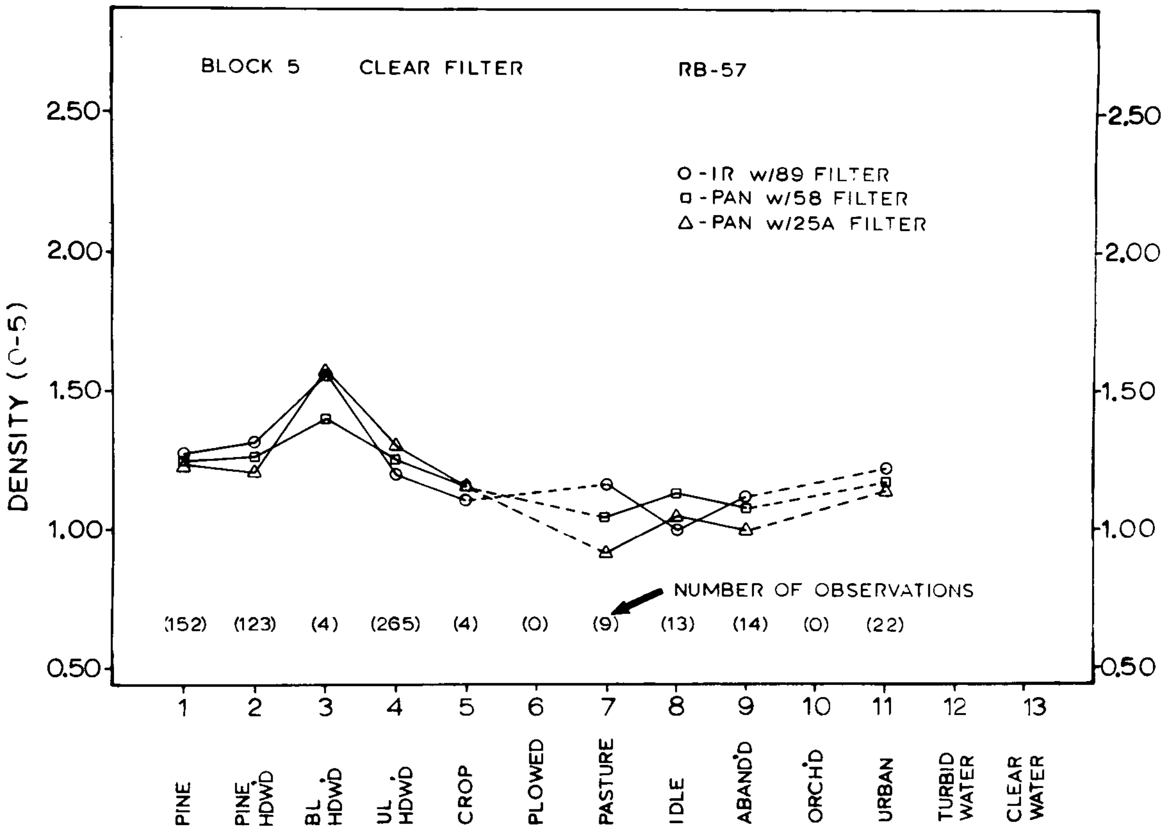

Figure 10.--The mean optical density (no filter) for 9 of 13 forest and nonforest classes on panchromatic (Wratten 25A), panchromatic (Wratten 58B), and B/W infrared (Wratten 89B)--Block 5 only.

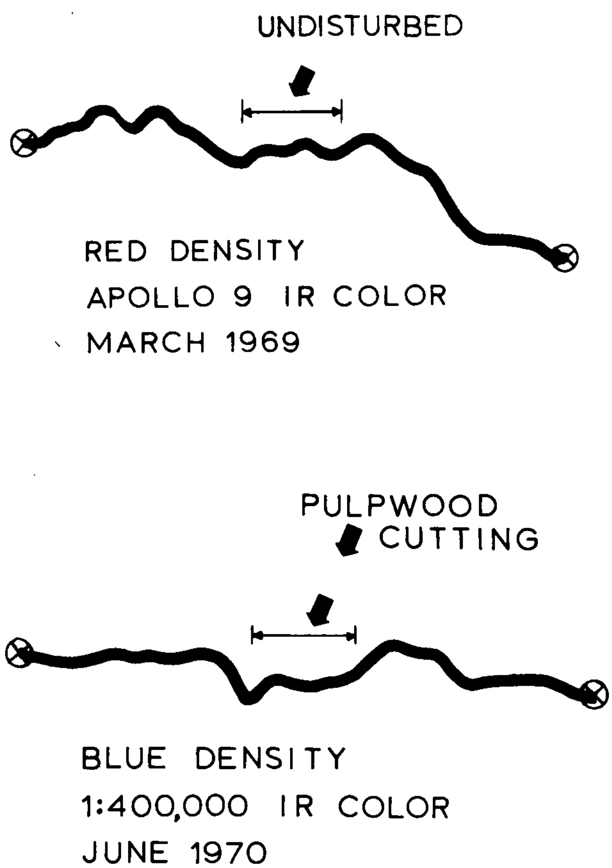

Figure 11A.--A pulpwood cutting that occurred sometime after the Apollo 9 mission, but before RB-57 Mission 131, is shown detected by a microdensitometer scan. The upper density trace was made using a red filter on the Apollo 9 IR color photograph. The lower density trace was made using a blue filter on the 1:420,000 scale IR color taken on the RB-57 Mission 131.

BEFORE CUTTING APRIL 1969

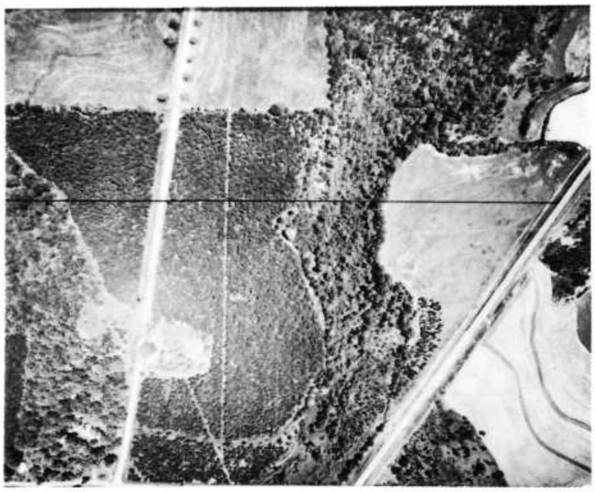

AFTER CUTTING MARCH 1970

Figure 11B.--The pulpwood cutting shown on the density trace in Figure 11A does not appear on the top photo taken in April 1969. A photograph (IR color) taken in March 1970, one year following Apollo 9, shows the pulpwood stand has been cut.

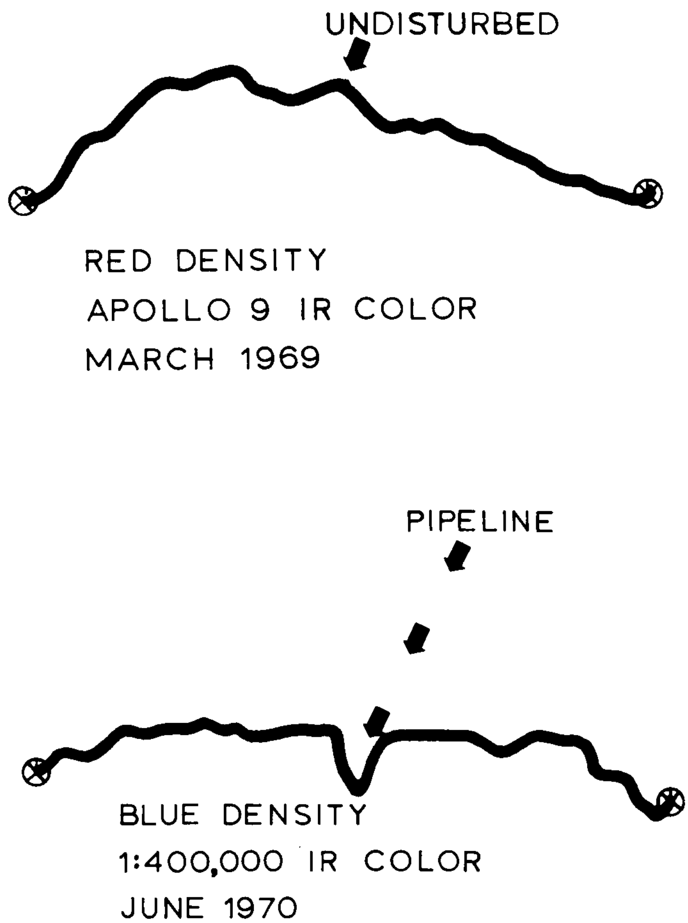

Figure 12A.--A pipeline that was constructed sometime after the Apollo 9 mission, but before RB-57 Mission 131, is shown detected by a microdensitometer scan. The upper density trace was made using a red filter on the Apollo 9 IR color photograph. The lower density trace was made using a blue filter on the 1:420,000 scale IR color photograph taken on RB-57 Mission 131.

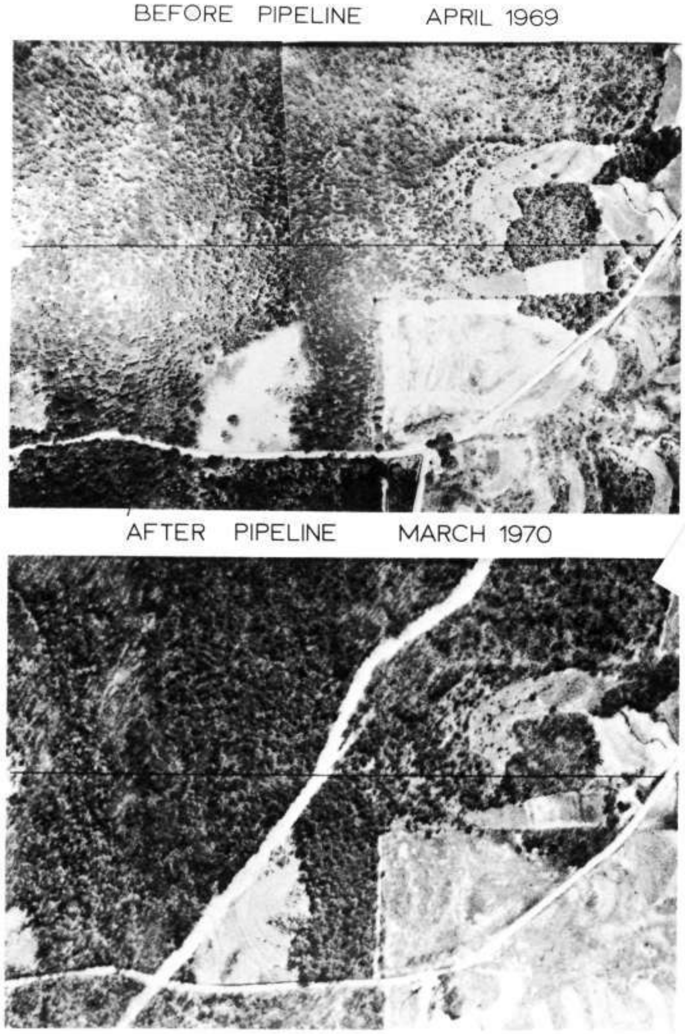

Figure 12B.--The pipeline shown on the density trace in Figure 12A does not appear on the top photo taken in April 1969. A photograph (IR color) taken in March 1970, one year following Apollo 9, shows the pipeline very clearly.